JOURNAL OF GEOPHYSICAL RESEARCH, VOL. 106, NO. D11, PAGES 11,859–11,874, JUNE 16, 2001

The stratospheric quasi-biennial oscillation in the NCEP reanalyses: Climatological structures

Amihan S. Huesmann and Matthew H. Hitchman

Department of Atmospheric and Oceanic Sciences, University of Wisconsin-Madison, Madison, WI

Abstract. Global quasi-biennial variation in the lower stratosphere and tropopause region is studied using 41 years (1958-1998) of reanalyses from the National Centers for Environmental Prediction (NCEP). Horizontal wind, temperature, geopotential height, tropopause temperature and pressure fields are used. A new quasi-biennial oscillation (QBO) indexing method is presented, which is based on the zonal mean zonal wind shear anomaly at the equator and is compared to the Singapore index. A phase difference compositing technique provides "snapshots" of the QBO meridional-vertical structure as it descends, and "composite phases" provide a look at its time progression. Via binning large amounts of data, the first observation-based estimate of the QBO meridional circulation is obtained. High-latitude QBO variability supports previous studies that invoke planetary wave–mean flow interaction as an explanation. The meridional distribution of the range in QBO zonal wind is compared with the stratospheric annual cycle, with the annual cycle dominating poleward of ~12° latitude but still being significant in the deep tropics. The issues of temporal shear zone asymmetries and phase locking with the annual cycle are critically examined. Subtracting the time mean and annual cycle removes ~2/3 of the asymmetry in wind (and wind shear) zone descent rate. The NCEP data validate previous findings that both the easterly and westerly QBO anomalous wind regimes in the lower stratosphere change sign preferentially during northern summer. It is noteworthy that the NCEP QBO amplitude and the relationships among the reanalyzed zonal wind, temperature, and meridional circulation undergo a substantial change around 1978.

1. Introduction

The stratospheric quasi-biennial oscillation (QBO) was first observed by *Reed et al.* [1961] and *Veryard and Ebdon* [1961]. An oscillation in the zonal wind at the equator, the QBO consists of zonally symmetric regimes of alternately easterly (from the east, hereafter designated "E") and westerly (hereafter "W") winds, which descend through the middle and lower stratosphere at a rate of ~1 km/month. The peak-to-peak range is ~42 m/s at the equator and decreases symmetrically away from the equator with a half width of ~12° latitude. Unlike the stratopause and mesopause semiannual oscillations (SAOs), this oscillation did not appear to be directly tied to the annual cycle, and its period was observed to be ~26 months. Now, with longer time series available, the average period has been shown to be ~28 months and ranges from just under 2 to ~3 years. Variability in the period renders interpretation of harmonic analyses of the QBO somewhat challenging [*Dunkerton and Delisi*, 1985]. Evidence has been given that supports the idea of a phase lock with the annual cycle [*Lindzen and Holton*, 1968; *Dunkerton and Delisi*, 1985, 1997], perhaps due to an interaction with the stratopause SAO. Here we examine the QBO as seen in the National Centers for Environmental Prediction/National Center for Atmospheric Research (NCEP/NCAR) reanalyses (hereafter "NCEP reanalyses") in light of observations made by these and other authors [e.g., *Reed*, 1965; *Reid and Gage*, 1985; *Dunkerton and Delisi*, 1985; *Yasunari*, 1989; *Pawson and Fiorino*, 1998b; *Randel et al.*, 1999]. We verify many of their observations and highlight new findings.

The first generally accepted theory of the QBO was presented by *Lindzen and Holton* [1968], who invoked the critical layer theory of wave–mean flow interaction to explain the QBO forcing by vertically propagating gravity waves. The initial theory was soon updated to favor exclusively the equatorial Kelvin and Rossby-gravity wave modes, interacting with the mean flow via infrared cooling so that they are damped out below the "critical level" [*Holton and Lindzen*, 1972]. An early laboratory experiment was remarkably successful in duplicating the main features of the oscillation and validated the theory that the QBO is driven by up-

Paper number 2001JD900031.
0148-0227/01/2001JD900031$09.00

ward propagating wave energy [*Plumb and McEwan*, 1978]. It is currently believed that gravity waves, as originally suggested by Lindzen and Holton, make a significant contribution to QBO forcing [*Alexander and Holton*, 1997; *Dunkerton*, 1997; *Politowicz and Hitchman*, 1997]. This has been shown to be true for the semiannual oscillation [*Hamilton and Mahlman*, 1988; *Hitchman and Leovy*, 1988]; however, the gravity wave spectrum is not sufficiently characterized to quantify their influence on the QBO.

The QBO is known to affect the temperature field and the transport of atmospheric constituents such as ozone, aerosols, HF, water vapor, N_2O, and CH_4 [*Lait et al.*, 1989; *Gray and Dunkerton*, 1990; *Zawodny and McCormick*, 1991; *Trepte and Hitchman*, 1992; *Hitchman et al.*, 1994; *Cordero et al.*, 1997; *O'Sullivan and Dunkerton*, 1997; *Randel et al.*, 1998] through a secondary meridional circulation that is integral to the theoretical model of the QBO [*Lindzen and Holton*, 1968; *Plumb and Bell*, 1982; *Dunkerton*, 1985]. The QBO circulation requires that a W shear zone be accompanied by a warm temperature anomaly created by convergence aloft, subsidence and warming at the equator, divergence below, and upwelling and cooling off the equator. The energy necessary for this thermodynamically indirect circulation comes from the wave driving of the QBO. Although the indirect signatures of this circulation have been detected, the small meridional velocities involved (~10 cm/s) and large errors in upper air wind data (~1 m/s) mean that the detection of a distinct QBO signal in the meridional wind itself has remained elusive. Wind data from sparsely distributed stations may yield inconclusive results [e.g., *Groves*, 1975]. Furthermore, constituent concentrations are not controlled solely by the QBO, so it may be difficult to interpret QBO-like signals in such data [*Gray and Dunkerton*, 1990; *Tung and Yang*, 1994a, 1994b]. This paper presents the first look at the meridional circulation of the QBO in a global meteorological data set.

There have been quasi-biennial components found in a number of tropospheric phenomena such as rainfall in various regions [*Gray*, 1984; *Kane*, 1995; *Whitney and Hobgood*, 1997], seawater temperatures [*Kawamura*, 1988; *Yasunari*, 1989], and the Walker circulation and El Niño-Southern Oscillation (ENSO) [*Gray et al.*, 1992b; *Knaff*, 1992; *Angell*, 1992]. Some of these are faint at best and are not generally accepted [*Kane*, 1992; *Xu*, 1992]. The present study was initiated to explore the possibility that the QBO affects tropical convection by modulating the cloud top environment [*Collimore et al.*, 1998]. Thus the focus of this paper is on the tropical tropopause region and lower stratosphere. The tropical tropopause is also important because it is one of the major ways for tropospheric air to enter the stratosphere [*Newell and Gould-Stewart*, 1981; *Doherty et al.*, 1984].

In the following section the data set and methods of analysis used in this study are described. Section 3 examines some characteristics of the annual cycle and QBO in zonal wind. The QBO index used in this study is different from those commonly used and is discussed in Section 4. Section 5 contains a description of the meridional structure of the stratospheric QBO in NCEP reanalysis zonal wind, temperature, geopotential height, meridional wind, and tropopause temperature. The time progression of the zonal average QBO in the vertical (on the equator) and on a single constant pressure surface is examined in Section 6. Conclusions, possible implications, and directions for future study are discussed in the final section.

2. Data and Methodology

2.1. The NCEP Reanalyses

The data used in this study are from the NCEP reanalyses, obtained from the National Oceanic and Atmospheric Administration–Cooperative Institute for Research in Environmental Sciences Climate Diagnostics Center in Boulder, Colorado (www.cdc.noaa.gov). The reanalysis, begun in 1991, was intended to address the problem of apparent climate changes in long-term data sets due to changes in the data assimilation system [*Kalnay et al.*, 1996; *Kistler et al.*, 2001]. Data from many different sources (including rawinsondes, balloons, aircraft, ships, surface stations, and satellites) were put through a quality check, fed into an assimilation model that includes parameterizations for all major physical processes, and finally examined again for self-consistency. The NCEP reanalyses now cover the years from 1948 to the present; in this study the 41 years 1958-1998 were used. Because of the large quantity of data and the timescales of interest, monthly averages were calculated from daily data prior to analysis. Monthly anomalies were obtained by subtracting the 41-year climatological mean for that month from the monthly average.

The NCEP fields have been "graded" according to the relative influence of the observed data and the assimilation model on the output field. Class A fields are highly influenced by observations (e.g., horizontal winds), class B fields are directly affected by observations but are influenced by the model (e.g., pressure vertical wind), class C fields are solely derived from the model (e.g., cloud positions), and class D fields are obtained from climatological values and are not affected by the model (e.g., land-sea mask). For example, while the meridional wind is a class A field, the vertical wind is a class B field. Thus the mean meridional circulation is best regarded as a class B field, determined by a mixture of observations and dynamical balance constraints of undetermined relative weighting.

All data are given on a 144 x 73 global grid. The constant pressure level (temperature, geopotential height, zonal and meridional winds) and tropopause (pressure and temperature) fields used in this study are all class A fields. The 17 constant pressure levels are: 1000, 925, 850, 700, 600, 500, 400, 300, 250, 200, 150, 100, 70, 50,

30, 20, and 10 hPa. The tropopause was defined as the lowest level (between 450 and 85 hPa) at which the temperature lapse rate is < 2 K/km. Since the highest level of the reanalysis is at 10 hPa, it does not capture the upper portion of the QBO and may suffer from unrealistic model boundary conditions. In addition, the introduction of satellite data into the assimilation is coincident with some abrupt changes in the characteristics of the data [*Pawson and Fiorino*, 1999; *Randel et al.*, 2000].

2.2. Indices and Compositing Methods

Since it takes one phase of the QBO many months to descend and the QBO variation is superimposed on the annual cycle, characterization of a given month as W phase or E phase depends strongly on one's research goals and perspective. For example, the winds at 20 hPa may be W while those at 50 hPa are E, or the anomalous wind may be W while the raw wind is E. Many previous studies have keyed on the time series or anomalies of the zonal wind at Singapore or other stations [*Garcia and Solomon*, 1987; *Lait et al.*, 1989; *Kane*, 1995; *Kinnersley and Pawson*, 1996; *Kinnersley and Tung*, 1999; *Randel et al.*, 1999] largely because of the availability and consistency of single station data [*Naujokat*, 1986; *Andrews et al.*, 1987; *Holton*, 1992]. Some have used the zonal wind shear at Singapore [*Gray et al.*, 1992b; *Hitchman et al.*, 1994], some have used a zonal average wind series [*Gray*, 1984; *Gray and Ruth*, 1993], and some have used combinations thereof [*Gray et al.*, 1992a]. Many do not state explicitly how the authors have defined the E and W phases.

Here we use NCEP reanalysis zonal mean equatorial zonal wind ($\overline{u}_{\mathrm{eq}}$) shear anomaly time series as QBO indices. The primary index is the wind shear in the lowest stratospheric layer (50-70 hPa) and is useful for studying near-tropopause variations. Figure 6 compares this index with the 50-70 hPa anomalous shear at Singapore. Similar indices are also defined for the three upper layers (10-20, 20-30, and 30-50 hPa).

To investigate the possibility of a "phase lock" with the annual cycle, a compositing method similar to that of *Yasunari* [1989] was followed in Figure 5. This is the only analysis herein that does not employ a shear anomaly index. The 50 hPa $\overline{u}_{\mathrm{eq}}$ anomaly is used for comparison to *Dunkerton and Delisi* [1985]. Specifically, for each full QBO cycle in the NCEP data set (16 total), the month when the 50 hPa $\overline{u}_{\mathrm{eq}}$ anomaly experienced a transition (E to W or W to E) was labeled. A composite W to E (E to W) year is then calculated by averaging over 16 years in which W to E (E to W) transitions occur. For example, W to E transitions occur in May 1960, July 1962, June 1965, and so on. The February vertical profile for the composite W to E year is the average of the vertical profiles for February 1960, February 1962, February 1965, and so on.

The four shear indices are used to generate time-lapse "snapshots" of the structure of QBO features by averaging anomalies according to W and E phases and by calculating "W minus E" differences (Figures 8-10 and 12-15). By looking in succession at fields binned according to the 10-20, 20-30, 30-50, and 50-70 hPa indices, four successive relative times in the QBO cycle can be examined. The strength of using this method with such a long data record can be illustrated as follows. Assuming a random error distribution and similar uncertainties for each of N measurements, the uncertainty of an average goes as $1/\sqrt{N}$ [*Bevington and Robinson*, 1992]. Thus, the uncertainty in a W minus E difference (a composite of 391 months) is reduced to 5% ($1/\sqrt{391}$) that of a single monthly average, which in turn will have an uncertainty 18% ($1/\sqrt{30}$) that of a daily average.

Although the structures are qualitatively well represented by a W (or E) average using this method, it does not capture an absolute amplitude since it effectively averages over most of a half cycle (a span of $\sim$1 year). This method also eliminates some of the more subtle phase relationships of the QBO. To investigate these subtleties and examine the more precise time evolution of the QBO, "composite time series" (after *Dunkerton and Delisi* [1985]) are calculated (Figures 16 and 17). That is, for each complete phase of the QBO, the months when the QBO index went from being W to E and those when the index went from E to W were recorded. Composite 31-month time series were then constructed by averaging together 16 separate 31-month time series with the transition month positioned at "month zero." There is more uncertainty in such a composite than in a W minus E average; instead of averaging 391 months, only 16 months are averaged for each point. Note that this method is different from that used to examine the phase lock with the annual cycle. Here the transition month of each individual series is placed at the same time in the composite (month zero), whereas in the method used to produce Figure 5, the transition may occur at any month in the composite.

A similar method was used to calculate the average QBO range in Figure 4. For each latitude-pressure point, composite $\overline{u}$ anomaly time series are constructed for each of the four indices (W to E and E to W; a total of 8 series). All four indices are used because the QBO is not strictly periodic, so levels not adjacent to the index layer may have somewhat degraded amplitudes. The difference between the maximum and minimum values in these series is taken to be the QBO range for that point.

3. The QBO and the Annual Cycle

Figure 1 shows a time-pressure section of $\overline{u}_{\mathrm{eq}}$. Features of the QBO that are immediately evident are as follows: the zonal wind at all stratospheric levels oscillates between E and W (with $\overline{u}_{\mathrm{eq}}$ ranging from ~ -35 to 15 m/s), the phase of the oscillation propagates downward, the E regime lasts longer than the W above $\sim$50 hPa and propagates slower than the W, and the aver-

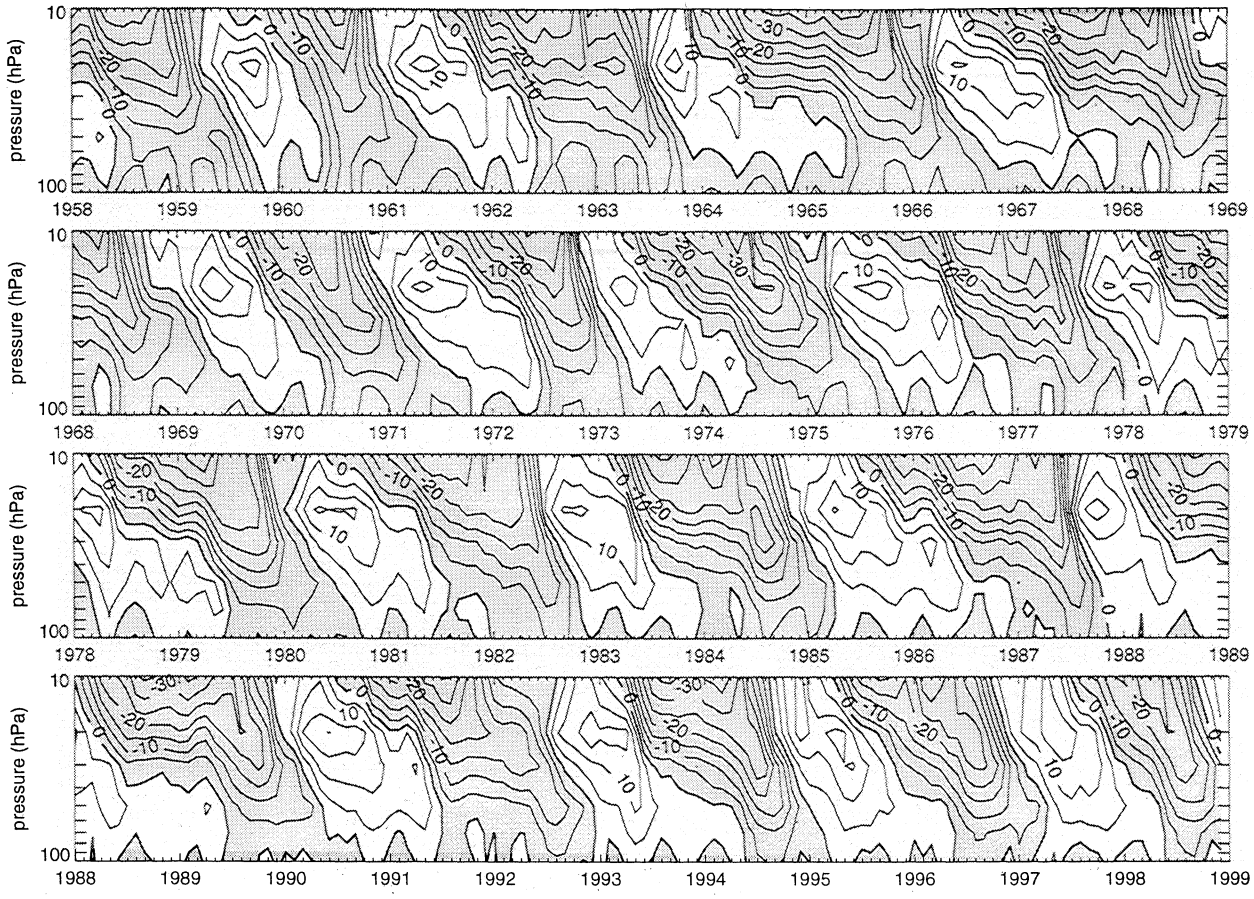

Figure 1. Zonally averaged equatorial zonal wind ($\overline{u}_{eq}$) as a function of time and pressure. Each panel contains 11 years of data, so that 3 years (1968, 1978, and 1988) are plotted twice. Dates on the x axis indicate the January of that year. Contour interval is 5 m/s. Negative values are lightly shaded, and the zero contour is thickened.

age period of this oscillation is ~28 months (but has a range of ~22-36 months).

The annual cycle in $\overline{u}_{eq}$ is shown in Figure 2 and can be compared to the annual cycle at Singapore [Figure 5 of *Hitchman et al.*, 1994]. The northern summer E maximum in the upper troposphere is associated with the Tibetan high [*Hitchman et al.*, 1997], which is strong at Singapore and dominates the zonal average. Note that the time and zonal mean shear is W between ~200 and 70 hPa and increasingly E above ~50 hPa. In contrast, the shear at Singapore is E in the upper troposphere, strongly W across the tropopause, E in the stratosphere, and W again above 20 hPa during northern spring and summer. Singapore also exhibits a thin time mean W wind layer just above the tropopause, which is not observed elsewhere [*Yao*, 1994].

When the annual cycle and time mean are removed from the raw data, the two wind regimes are more equal in duration and in rate of descent (Figure 3), but these asymmetries are not completely removed (discussed quantitatively in Section 6.1). While Singapore's annual cycle is clearly different from the zonal average, removal of the annual cycle at any individual station does not completely remove the zonal asymmetry, either.

Figure 4 compares the average ranges in $\overline{u}$ for the annual and QBO cycles in the NCEP reanalyses. The shading indicates the approximate region in which the QBO range exceeds the annual cycle range, essentially within 12° of the equator and above the tropopause.

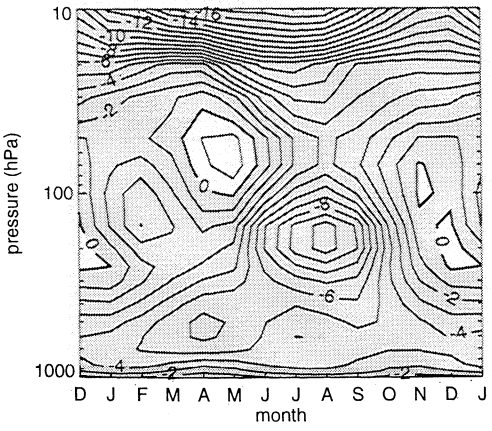

Figure 2. Annual cycle of National Centers for Environmental Prediction (NCEP) $\overline{u}_{eq}$ anomaly as a function of pressure. For clarity, the first month plotted is December and the last is January. Contour interval is 1 m/s.

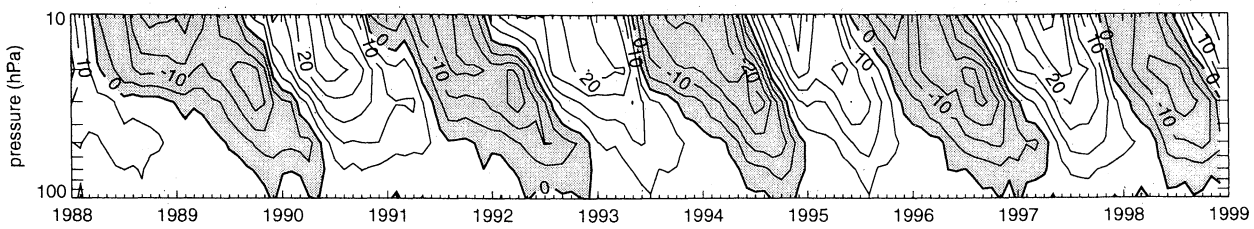

Figure 3. Same as Figure 1, but for the anomaly. To avoid repetition, only the last decade is shown. Contour interval is 5 m/s.

It is important to note that there may be a quasi-biennial signal in tropospheric winds that is not zonally symmetric [*Yasunari*, 1989; *Knaff*, 1992]. The QBO ranges and amplitudes are similar in the NCEP data, the European Centre for Medium-Range Weather Forecasts (ECMWF) operational data [*Trenberth*, 1992], the United Kingdom Meteorological Office (UKMO) data [*Randel et al.*, 1999], and earlier work by *Reed* [1965]. The annual cycle is a maximum near the subtropical tropopause jets and in the extratropical upper stratosphere (winter polar vortices), but is significant even in the equatorial stratosphere, exceeding 4 m/s (see Figure 2). The annual cycle in the Southern Hemisphere (SH) stratosphere is larger than in the Northern Hemisphere (NH) because of the more robust planetary wave activity in the NH [*Mahlman and Fels*, 1986]. The annual cycle of the subtropical jet is stronger in the NH than in the SH because of a larger-amplitude Hadley circulation during the northern winter [*Dunkerton*, 1989; *Holton et al.*, 1995]. The QBO range peaks in the tropics between 10 and 20 hPa. The high-latitude maxima (see Figure 4) may be due to the QBO modulation of planetary wave refraction, with stronger planetary waves in the NH accounting for the stronger maximum there. Yet in a 41-year data record it is still possible that some amount of interannual variability unrelated to the QBO is not filtered out via averaging by phase of the QBO.

Previous authors have pointed out a possible phase lock between the annual cycle and the QBO, whereby phase transitions tend to occur at the same time of year [*Lindzen and Holton*, 1968; *Wallace*, 1973; *Dunkerton and Delisi*, 1985; *Yasunari*, 1989]. Figure 5 illustrates two annual composites (W to E years and E to W years) of $\overline{u}_{\rm eq}$ anomaly, with the 6 months before and after that year included for continuity. The large amplitude seen here suggests that transitions tend to occur around the same time of year (during May-June for E onset at the 50 hPa level, in agreement with *Dunkerton and Delisi* [1985], and in July for W onset). This clustering of transition times is coherent in altitude, and the preferred month for a given level may be read from Figure 5.

4. A New QBO Index

Figure 6 shows the anomalous 50-70 hPa zonal wind shear for both the Singapore station and the NCEP zonal average. The latter is the primary QBO index. The shear is preferred over the wind values because it facilitates comparison of temperature, geopotential height, and zonal wind via the thermal wind relationship. For clearer distinction between phases, months when the shear is smaller than a certain value are considered to be "intermediate" months and are not included in any E or W averages. This "threshold" shear

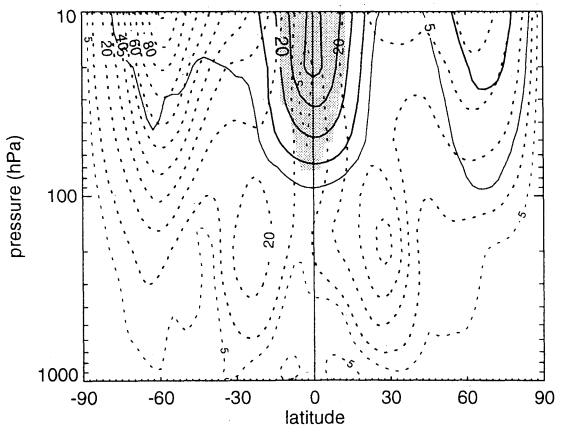

Figure 4. Average quasi-biennial oscillation (QBO) (solid contours) and annual cycle (dotted contours) ranges of $\overline{u}$ (maximum−minimum for one cycle). Contour interval is 5 m/s; the shaded region is approximately where the QBO range exceeds the annual.

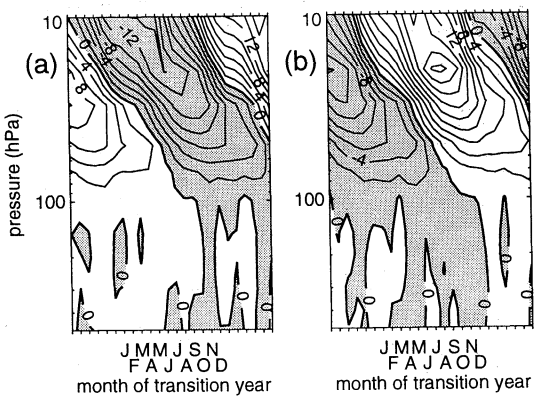

Figure 5. The $\overline{u}_{\rm eq}$ anomaly, averaged over 16 years in which (a) westerly (W) to easterly (E) and (b) E to W transitions took place in the 50 hPa $\overline{u}_{\rm eq}$ anomaly (see Section 2.2). For clarity, the 6 months before and after the transition year are included. Contour interval is 2 m/s.

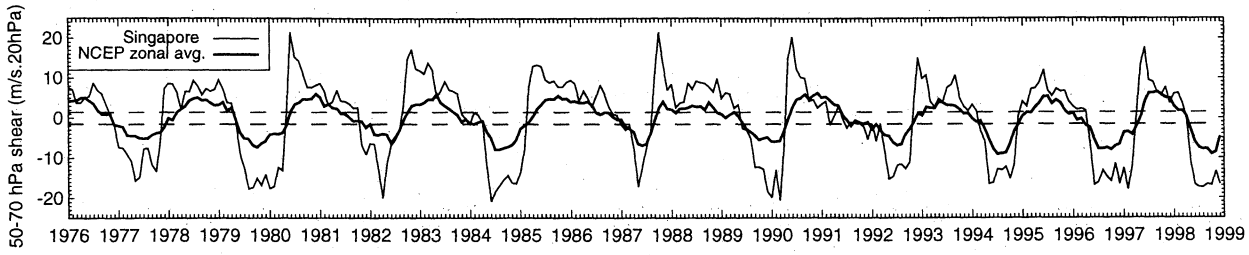

Figure 6. The 50-70 hPa NCEP $\overline{u}_{eq}$ shear anomaly (thick solid line) and Singapore 50-70 hPa shear anomaly (thin solid line) in m/s per 20 hPa as functions of time. The dashed lines indicate cutoffs for E and W phase differentiation for the QBO index.

was selected empirically to be 1.5 m/s per 20 hPa. Also, months when the shear "flip-flops" between regimes (for example, June-December of 1991) are considered to be intermediate. Using this method, the 492 months were divided into 101 intermediate months, 209 W months, and 182 E months. Similar indices were prepared for the upper layers (10-20, 20-30, and 30-50 hPa). The threshold shears for these indices were adjusted so that there is an equal number of intermediate months for each index. As expected from the fact that the E wind and wind shear regimes propagate downward more slowly than the W, the upper level indices have increasingly more E months and fewer W months.

One problem with using a single station's data as a QBO index is that the annual cycle in the zonal wind displays significant zonal asymmetries [Figure 2; *Yao*, 1994]. Figure 7 shows a Hovmöller diagram of the annual cycle of the 50-70 hPa u_{eq} shear and illustrates this asymmetry. Figure 8 shows the global W minus E 50-70 hPa zonal wind shear anomaly. This shows that the QBO anomalous shear is much more zonally symmetric than the annual cycle, although there are slight asymmetries that may be persistent and physically based [Figures 6 and 8; *Hitchman et al.*, 1997]. Since each station's annual cycle is quite different but the interannual anomalies are similar, a time series for one particular station will certainly not reflect the character of the QBO at all longitudes, a single station anomaly series will be appreciably better, and a zonal average anomaly will be the most universally applicable. In fact, NCEP has stopped offering the Singapore 30 and 50 hPa zonal wind series as QBO indices in favor of the respective equatorial zonal averages (www.cpc.ncep.noaa.gov/data/indices).

Figure 9a illustrates the meridional and QBO phase dependence of the $\overline{u}$ shear in the 50-70 hPa layer for the northern winter (December-January-February) season. Figure 9b shows the W and E $\overline{u}$ shear anomalies averaged over all seasons. Note the high-latitude effects: there is a secondary and opposite oscillation off the equator, and yet another oscillation farther north. This is negligible in the SH and is strongest during the northern winter.

5. "Snapshot" Evolution of the Meridional QBO Structure

5.1. Zonal Wind

The $\overline{u}$ anomaly was binned according to each of the four indices, and then the W minus E differences were calculated. These four successive latitude-pressure sections are shown in Figure 10. The extent of the QBO agrees with Figure 4, but the maxima are smaller because this method averages through half cycles. Note that between Figures 10a and 10d there seems to be almost precisely one half period of the QBO oscillation:

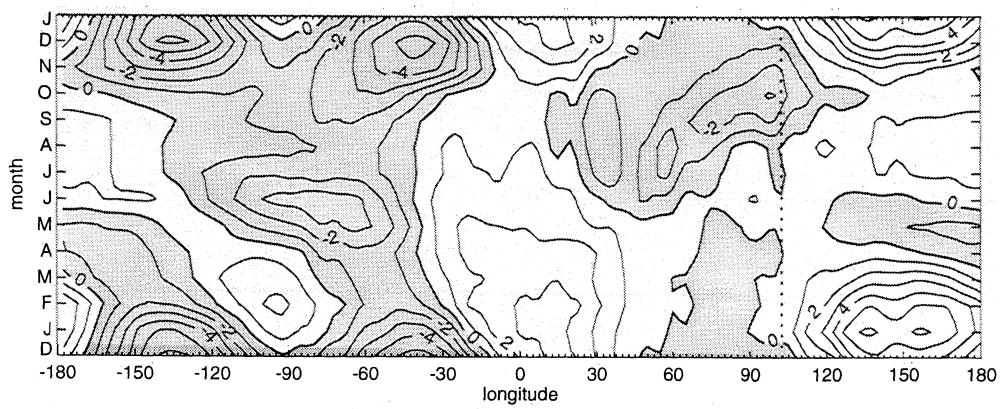

Figure 7. Annual cycle of the 50-70 hPa u_{eq} shear as a function of longitude. Singapore's longitude is marked by a dotted line. Contour interval is 1 m/s per 20 hPa.

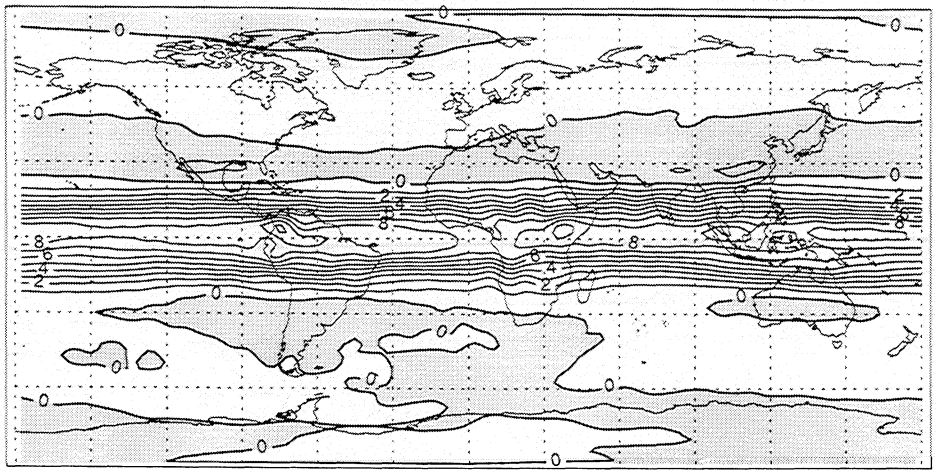

Figure 8. Longitude-latitude plot of the 50-70 hPa anomalous zonal wind shear, W average minus E average. Contour interval is 1 m/s per 20 hPa.

the E regime in Figure 10a is almost exactly the same strength and at the same location as the W regime in Figure 10d (this is also seen in Figures 11-14). Also apparent is a perturbation in the region of the north polar stratospheric vortex, as in Figure 4. This feature may be a result of the properties of planetary wave interaction [*Holton and Tan*, 1980; *O'Sullivan and Salby*, 1990; *Chen and Huang*, 1999]. These waves are generated near or below the tropopause and propagate upward through weak to moderate W winds until they "break" in the stratosphere, causing turbulence and irreversible mixing. This tends to disturb the coherence of the vortex in the winter and is the cause of "sudden" stratospheric warmings. When there is an E anomaly in the tropics, the waves tend to propagate mostly upward; and when there is a W anomaly in the tropics, they tend to refract equatorward, away from the vortex. Therefore we would expect a stronger, colder vortex during the W phase, when the waves break farther away from the vortex (Figures 10d, 12d, and 13d).

The vertical dependence of lag correlation for QBO shear and 10 hPa heights over the north pole is illustrated in Figure 11. The correlation is significant, mostly because it is periodic with respect to lag, with a period of about that of the QBO. The progression downward can be seen by comparing the lines in Figure 11 (from thinnest to thickest) to Figures 10a-d, 12a-d, and 13a-d. When anomalous shear is W in the 10-20 hPa layer (E winds in the equatorial lower stratosphere), the north polar stratosphere is warmer and thicker (thinnest line in Figure 11; Figures 10a, 12a, and 13a); when shear is W in the 50-70 or 30-50 hPa layers (W winds in the lower stratosphere), the lower stratosphere is colder and thinner (thickest line in Figure 11; Figures 10d, 12d, and 13d).

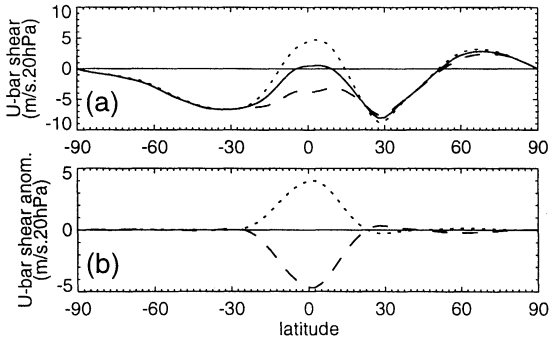

Figure 9. (a) Northern winter (December-January-February) W (dotted line), E (dashed line), and climatological (solid line) 50-70 hPa $\overline{u}$ shear as a function of latitude. (b) W anomaly (dotted line) and E anomaly (dashed line) annual averages.

5.2. Temperature and Geopotential Height

The zonally averaged temperature anomaly at the equator, according to the thermal wind relationship [e.g., *Holton*, 1992], should be positive ($\partial^2\overline{T}'/\partial y^2 < 0$) when the shear anomaly is positive ($\partial\overline{u}'/\partial z > 0$) and negative when the shear anomaly is negative:

$$\frac{\partial\overline{u}'}{\partial z} = \frac{-g}{f\,\overline{T}}\frac{\partial\overline{T}'}{\partial y} \approx \frac{-g}{\beta\,\overline{T}}\frac{\partial^2\overline{T}'}{\partial y^2}, \qquad (1)$$

where the right hand approximation applies near the equator, g is the gravitational acceleration, z is the geopotential height, y is the meridional dimension on a β-plane, f is the Coriolis parameter, and β is the variation of f with respect to meridional dimension ($\partial f/\partial y$). Primed quantities indicate anomalies and overbars indicate zonal averages.

The zonally averaged wind and temperature anomalies (Figures 10 and 12) agree with equation 1 almost exactly (also seen in the UKMO analyses by *Randel et al.* [1999]). One general exception is that the temperature perturbation seems to extend somewhat lower than the wind perturbation, i.e., below 100 hPa. A distinct node exists near ±15° latitude, with the subtropical oscillation being opposite in phase and having

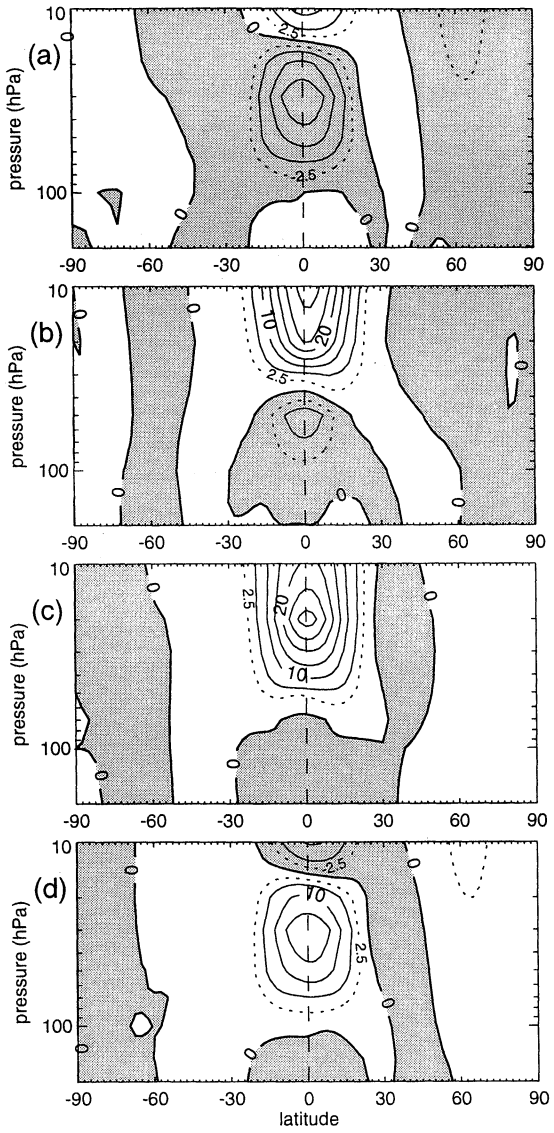

Figure 10. Latitude-pressure sections of the W minus E $\overline{u}$ anomaly for the (a) 10-20, (b) 20-30, (c) 30-50, and (d) 50-70 hPa indices. Contour interval is 5 m/s with additional, dotted contours at ±2.5 m/s.

a strength ~1/4-1/2 that of the equatorial. This oscillation is clearly stronger in the NH. While there may be a seasonally based hemispheric asymmetry, these results show consistently larger anomalies in the NH (also observed by *Randel et al.* [1999]).

The zonally averaged geopotential height anomaly is shown in Figure 13. Again, the meridional node is distinct. The strength of the off-equator oscillation is ~1/4-1/3 that on the equator. Because of a generally deeper temperature perturbation at high latitudes, the height perturbation can be larger at the pole than it is at the equator. There is also an apparent tendency (Figures 13a, 13c, and 13d) at the equator for a strong perturbation just above the tropopause to be accompanied by a weaker, opposite perturbation just below the tropopause. This tropopause "node" will be examined further in Section 6.1.

Using the hydrostatic relationship between the bounding pressures and thickness (Δz) of a layer, a perturbation thickness is

$$\Delta \overline{z}' = \frac{R\overline{T}'_{\text{ave}}}{g} \, ln\left(\frac{P_{\text{bottom}}}{P_{\text{top}}}\right) . \qquad (2)$$

Thus, a perturbation height will be the sum of the perturbation layer thicknesses or temperatures below that level. Equivalently, where the temperature (or shear) perturbation is positive, the height perturbation will increase with height and vice versa. Extrema of the height perturbations tend to be at the same levels where the temperature perturbations are zero. This is followed quite closely in Figures 12 and 13.

5.3. Meridional Circulation

The temperature perturbations discussed in Section 5.2 can be thought of primarily as a result of vertical motion and the resultant cooling or warming. A warm anomaly, for example, is the result of air that has been forced downward. Areas of downwelling (warm anomalies) can thus be thought of as "quadrupoles" of meridional circulation, with convergence aloft and divergence below. While there has been very convincing indirect evidence of this circulation in the form of constituent concentrations [*Zawodny and McCormick*, 1991; *Trepte and Hitchman*, 1992; *Hitchman et al.*, 1994; *Cordero et al.*, 1997; *O'Sullivan and Dunkerton*, 1997; *Randel et al.*, 1998], little direct observational evidence has been produced, largely because of the very small meridional and vertical wind speeds involved.

These meridional wind quadrupoles can be seen clearly in Figure 14. For example, in Figure 14a the region of positive temperature anomaly (above 30 hPa) exhibits convergence aloft and divergence below, indicative of downwelling. The region of negative temperature anomaly (below 30 hPa in Figure 12a) exhibits divergence aloft and convergence below, indicative of upwelling. The magnitudes are comparable to those expected by models [e.g., *Kinnersley*, 1999], but the near-tropopause noisiness may be due to problems with the reanalyzed data [*Pawson and Fiorino*, 1998a;

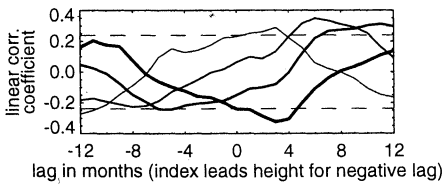

Figure 11. Linear correlation coefficient between the QBO shear indices and the North Pole 10 hPa geopotential height anomaly as a function of lag. The thickest line is for the 50-70 hPa index; progressively thinner lines are for progressively higher level shear indices. The dashed lines indicate the correlation coefficients above which there is a <1% probability that the data are completely uncorrelated [*Bevington and Robinson*, 1992].

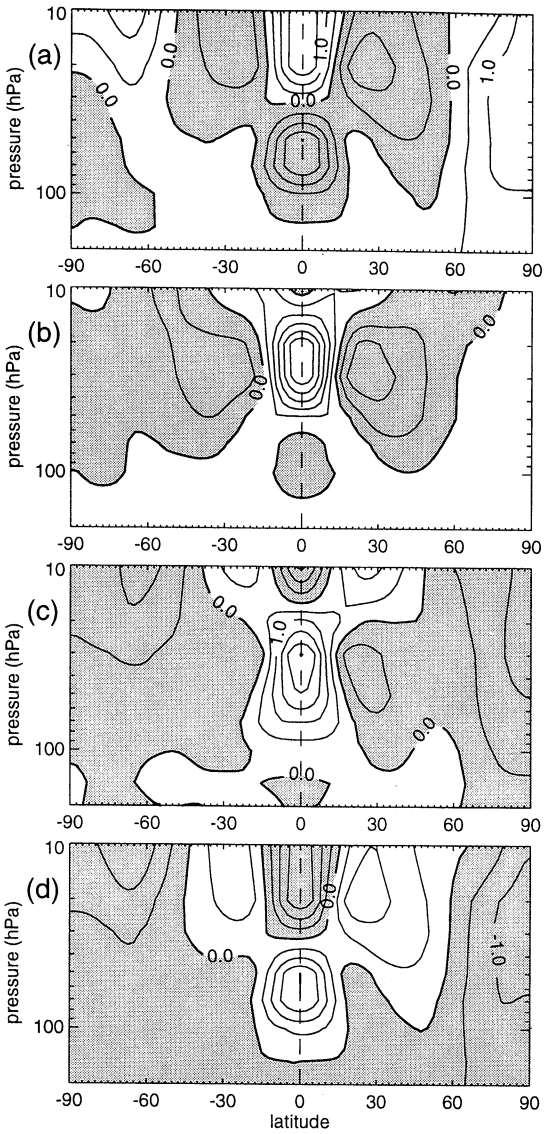

Figure 12. Same as Figure 10, but for the zonally averaged temperature anomaly. Contour interval is 0.5 K.

1999]. There is a clear hemispherical asymmetry in the strength of the meridional circulation; the NH meridional wind and temperature anomalies are stronger in each panel of Figures 12 and 14. The vertical motion field (as calculated from the temperature and meridional wind fields, not shown) indicates a peak-to-peak QBO range of ~4 mm/s at 10 hPa, with the maximum above 10 hPa. This is of the same order but generally larger than those calculated from other data [*Cordero et al.*, 1997; *Randel et al.*, 1999] or modeled [e.g., *Plumb and Bell*, 1982; *Politowicz and Hitchman*, 1997].

Here it is especially evident that although the actual perturbations may be much smaller than their uncertainties, using 391 months of data greatly decreases the uncertainty in the average and smoothes out much of the random variability. In the stratosphere, where daily measurements of horizontal wind speeds may have uncertainties of > 1 m/s; using (391 months) x (30 days) of data reduces this to > 1 cm/s (taking a zonal average reduces this even more). The fact that a time series of the reanalyzed meridional wind data shows much less coherence than, for example, a time series of the reanalyzed temperature data suggests that dynamical balance constraints may not be the primary generator of this signal. However, their precise influence relative to that of the input observations is not known.

5.4. The Tropopause

The link between the stratospheric QBO and tropical convection and rainfall is not yet fully understood [*Gray et al.*, 1992b; *Knaff*, 1992] and, indeed, not yet shown to be significant [*Collimore et al.*, 1998]. There are several possible mechanisms linking the stratospheric QBO and tropical convection. The cloud top environment may influence the strength of convective systems in several ways: modulation of the tropopause height (allowing for more or less vertical "room" and colder or warmer

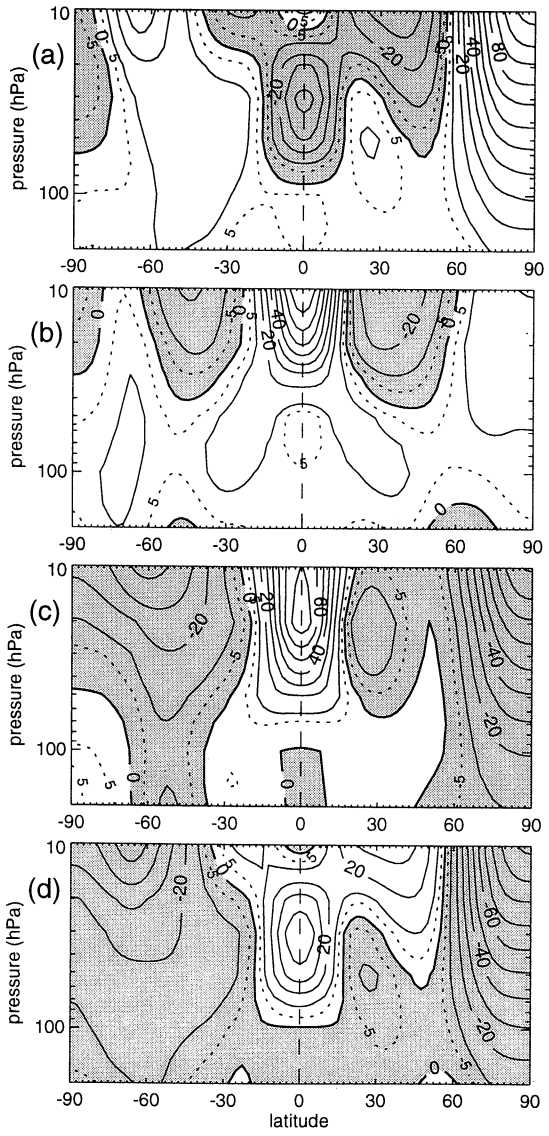

Figure 13. Same as Figure 10, but for the zonally averaged geopotential height anomaly. Contour interval is 10 m with additional, dotted contours at ±5 m.

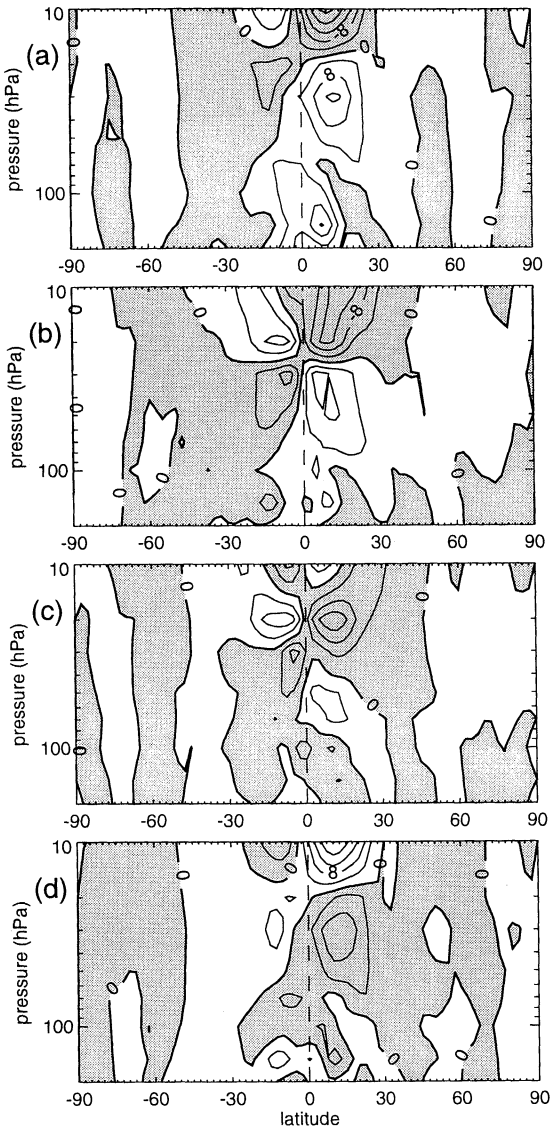

Figure 14. Same as Figure 10, but for the zonally averaged meridional wind anomaly. Contour interval is 4 cm/s.

cloud tops), the wind shear (more shear would tend to suppress coherence), or the inertial stability (which may enhance or inhibit outflow from the upper levels). The QBO may also shift the positions of convective centers. Exploring all of these mechanisms in detail is not the focus of this study; it does, however, highlight the importance of the tropopause QBO. The authors and their collaborators are preparing a manuscript detailing these results.

If the lowest layer of the stratosphere warms, such as occurs during the W phase, the tropopause should be lower and warmer; similarly, during the E phase the tropopause should be cooler and higher. Figure 15 supports the theoretical relationship between QBO phase and tropopause temperature and pressure. At the equator the tropopause is lower (higher) and warmer (cooler) during the W (E) phase, and there is an apparent node at $\sim \pm 20°$. Near the north pole there is an opposite oscillation. These observations agree with Figure 12d.

6. Composite QBO Time Series

Because of the inherent noisiness of a time series and the variability from phase to phase exhibited by the QBO, it is difficult to draw quantitative or even qualitative conclusions about a "typical" cycle of the QBO. However, some general statements can be made, and knowing what a typical cycle consists of may be valuable to both our theoretical understanding and our predictive abilities. Composite QBO cycles in equatorial vertical profile and on a constant pressure level surface (30 hPa) are presented in this section. For easier intercomparison between Figures 16 and 17, the transitions for the 30-50 hPa index were used for both.

6.1. Vertical Structure at the Equator

Figures 16a and 16b show composite QBO cycles for the W to E and E to W phase transitions, respectively, for the $\overline{u}_{eq}$ anomaly and zero shear anomaly lines (dotted). Regions away from the 30-50 hPa layer at month zero may have amplitudes degraded somewhat. The maximum range in $\overline{u}_{eq}$ anomaly is ~ -19 to 23 m/s and occurs between 10 and 20 hPa (see Figure 4) while that for $\overline{u}_{eq}$ shear (not shown) is ~ -4.2 to 5.5 m/s per kilometer and occurs in the 20-30 hPa layer. From the annual cycle in $\overline{u}_{eq}$, where both wind and wind shear are increasingly E with altitude above about 50 hPa, one would expect the E regimes to last increasingly longer with altitude or, equivalently, to descend slower than the W regimes. This is observed in the NCEP reanalyses. At the upper levels, the E maxima are shallower (weaker and less abrupt) than the W, so they last longer. However, since the W regimes descend faster than the E, by the lower stratosphere the W regimes last longer. Because of this and other asymmetries, the QBO is best described by a peak-to-peak (rather than an absolute) amplitude.

That this descent rate asymmetry is still present in the anomalies is in accordance with previous observa-

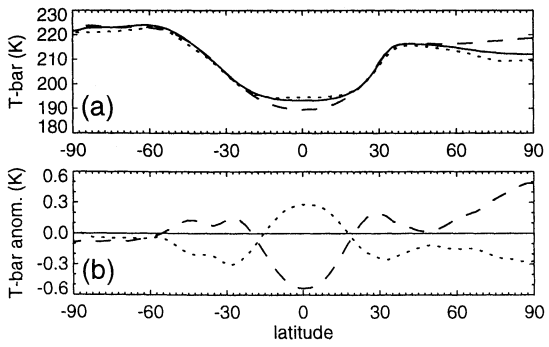

Figure 15. Same as Figure 9, but for the zonally averaged tropopause temperature (K). Deviations from climatology in Figure 15a are exaggerated by a factor of 5 for clarity.

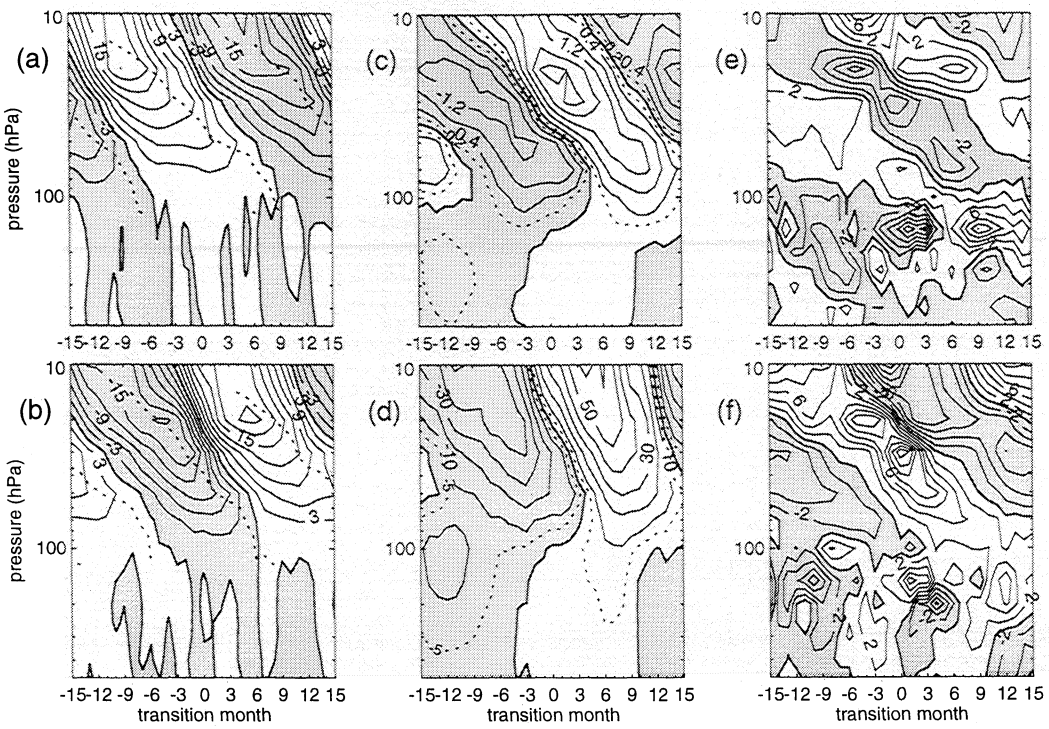

Figure 16. (a) W to E and (b) E to W transitions (keying on the 30-50 hPa index) for the $\overline{u}_{eq}$ anomaly. Contour interval is 3 m/s. The stratospheric zero shear lines are dotted. (c) Same as Figure 16b, but for the temperature anomaly, smoothed prior to averaging with a 3-month running mean. Contour interval is 0.4 K with additional, dotted contours at ±0.2 K. (d) Same as 16c, but for the pressure level height anomaly. Contour interval is 10 m with additional, dotted contours at ±5.0 m. (e) Same as Figure 16c, but for the zonally averaged meridional wind anomaly at 10°N. Contour interval is 2 cm/s. (f) Same as Figure 16e, but at 10°S.

tions and theoretical considerations. Since downwelling occurs where there is W shear and upwelling occurs where there is E shear, downward propagation of W shear is enhanced by vertical advection, whereas downward propagation of E shear is suppressed, as suggested by *Lindzen and Holton* [1968]. Here the W (E) $\overline{u}_{eq}$ regime takes ~7.9 (12.7) months to descend from 10 to 70 hPa whereas the anomalous $\overline{u}_{eq}$ regime takes ~9.1 (10.7) months. The W (E) $\overline{u}_{eq}$ shear regime takes ~9.8 (23.5) months to descend from the 10-20 hPa layer to the 70-100 hPa layer whereas the anomalous $\overline{u}_{eq}$ shear regime takes ~13.9 (17.9) months. Thus ~2/3 of the asymmetry (measured as the rate difference divided by the average rate) in wind and wind shear descent rate is removed upon subtraction of the annual cycle.

The regions of W shear in Figure 16b correspond to regions of warm anomaly in Figure 16c. Here there is a much more pronounced upper tropospheric signal. It is unclear whether the stratospheric and tropospheric anomalies are out of phase (as suggested in Section 5.2) or if the tropospheric anomaly propagates upward. This feature may be a result of balance constraints within the model, or it may be a residual of a zonally asymmetric tropospheric QBO signal [*Yasunari*, 1989]. The stratospheric temperature anomalies agree well with the shear anomalies. From Equation 1 (with a meridional scale of ~1000 km and an average layer temperature of ~220 K) the maximum shear values above imply temperature anomalies of ~ −2.2 to 2.8 K. The range of temperature anomalies here is ~ −1.7 to 2.6 K, similar to, but slightly smaller than, that calculated from the shear maxima.

The tropospheric structure of height anomalies in Figure 16d is similar to that seen in the temperature anomalies. There is good agreement with Figure 16c: where the temperature anomaly is positive, the height anomaly increases with height; and where the temperature anomaly is negative, the height anomaly decreases with height. Equivalently, it can be seen that where the temperature anomaly is zero, the height anomaly contours are vertical. The apparent tropopause "node" in Figure 13 is seen here to be the result of a more complex phase relationship between the upper troposphere and lower stratosphere. It appears at an altitude where the W minus E difference is zero because the oscillation is 1/4 cycle out of phase with the QBO index and not because there is no QBO variation.

Figures 16e and 16f illustrate the QBO meridional circulation. Qualitatively, they agree with Figure 16c: where the temperature anomaly is positive, the meridional wind exhibits equatorial convergence and vice versa. However, there is clearly a large amount of

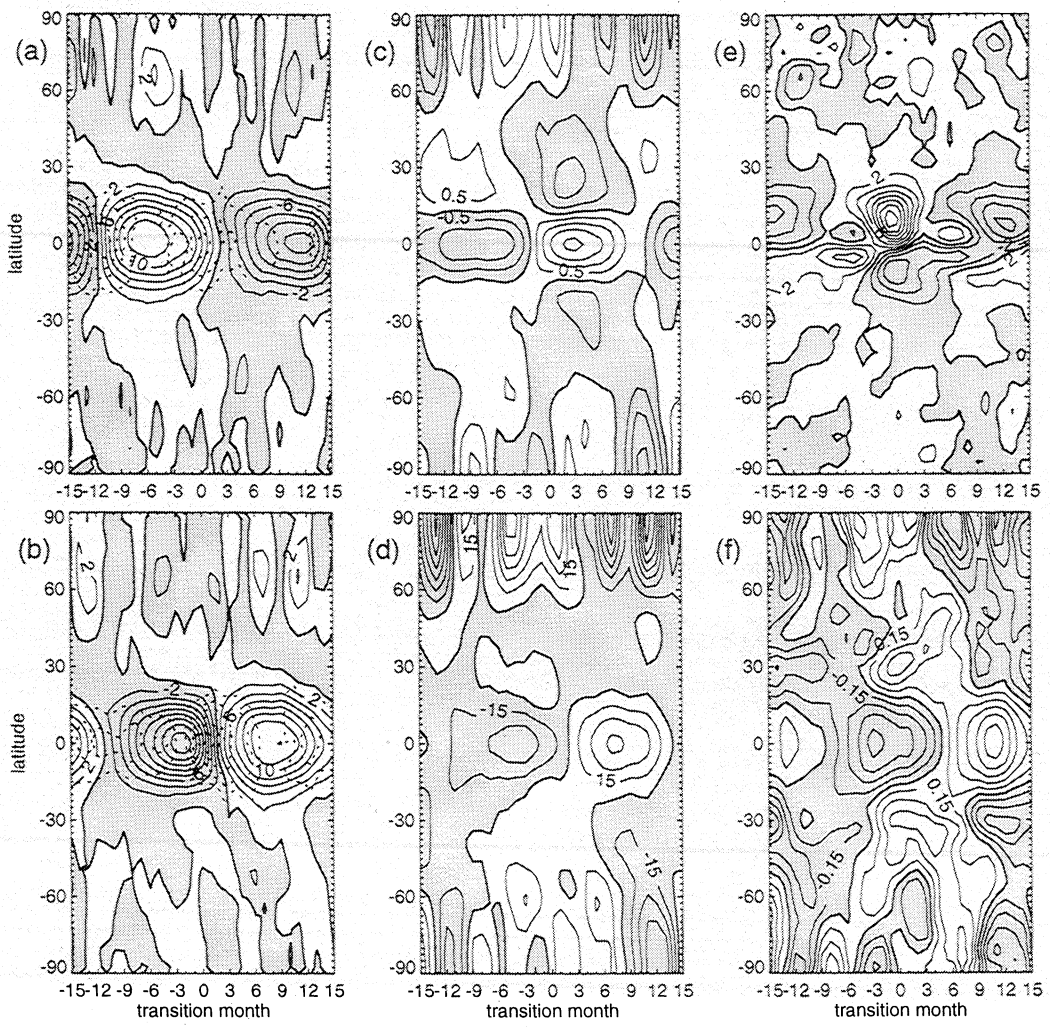

Figure 17. (a) W to E and (b) E to W transitions (keying on the 30-50 hPa index) for the 30 hPa $\overline{u}$ anomaly. Contour interval is 2 m/s. Dotted lines indicate acceleration contours at intervals of 1 m/s per month (m/s.month). For clarity, they are plotted only in the tropics and a zero contour is not plotted. (c) Same as Figure 17b, but for the 30 hPa temperature anomaly, smoothed prior to averaging with a 3-month running mean. Contour interval is 0.5 K. (d) Same as Figure 17c, but for the geopotential height anomaly. Contour interval is 15 m. (e) Same as Figure 17c, but for the meridional wind anomaly. Contour interval is 2 cm/s. (f) Same as Figure 17c, but for the zonally averaged tropopause temperature anomaly. Contour interval is 0.15 K.

noise in the data, and the NH circulation is stronger. The reanalyzed meridional wind suffers from mass balance problems discussed by *Pawson and Fiorino* [1998a; 1999]. The upper tropospheric noise may be a result of these inconsistencies, as the QBO binning does not remove other large interannual variations.

6.2. Meridional Structure

Figures 17a and 17b show the meridional variation of anomalous $\overline{u}_{eq}$ and $\overline{u}_{eq}$ acceleration (dotted contours) at 30 hPa for the QBO transitions. The acceleration contours show that the W acceleration is stronger and lasts for a shorter time. In addition, as observed by *Dunkerton and Delisi* [1985], the W acceleration exhibits one maximum at the equator, while the E exhibits a double-peaked character. This is seen at all stratospheric levels.

Hamilton [1984] and *Dunkerton and Delisi* [1985] also noted that the E acceleration tends to start simultaneously across the equator, while the onset of W acceleration is concentrated at the equator and spreads poleward. Figures 17a and 17b suggest that this may be true in the NCEP data as well. The anomalous wind regimes, on the other hand, do have distinctly different shapes: the E is "squarish," while the W is more "rounded" in Figures 17a and 17b. This feature is more prominent at the upper levels. *Hitchman et al.* [1994] show snapshots of this feature at 30 hPa in plan view, highlighting the zonal asymmetry in the ECMWF operational analysis data. Thus the QBO phases cannot be thought of as equal but opposite; they are asymmetric

in overall duration, downward and meridional propagation, acceleration (the E regime is double-peaked), and amplitude.

In both the temperature and geopotential height fields (Figures 17c and 17d) the oscillation near the north pole is observed to be ~3 months behind the 30-50 hPa index (it is approximately in phase with the 50-70 hPa index); Figures 17a and 17b show a stronger north polar vortex when the polar stratosphere is colder and thinner (little variation is seen in the south polar vortex). This phase relationship is true for all levels in the stratosphere, since the anomaly is related to planetary wave dynamics and affects the whole layer. While the subtropical oscillation is clear in the temperature field, it is much weaker in the geopotential height field.

To interpret Figure 17e, which shows the E to W transition for the meridional wind anomaly, we note that around the transition month there is a net divergence at the equator at 30 hPa. This implies that there is a region of downwelling (warm anomaly) above and a region of upwelling below. Since the pattern moves downward, this means that there is a cool anomaly before the transition month and a warm anomaly after, in agreement with Figure 17c. Qualitatively, the strength of both the meridional circulation and the extratropical temperature oscillation appears weaker in the SH.

Figure 17f shows the E to W transition for the tropopause temperature and calls into question the conclusions drawn previously about a meridional node. While the north polar oscillation appears to be in phase with the north polar oscillations in Figures 17c and 17d, this anomaly appears to move equatorward, with the extratropical E (W) maximum occurring ~3 months after the equatorial W (E) maximum. The nodes in Figure 15 (around ±20°) are indicative of a 1/4 cycle lag rather than a zero QBO variation. There is an equatorial peak-to-peak variation of ~1.2 K and ~3.4 hPa in the tropopause temperature and pressure, respectively; the pressure variation corresponds to a height variation of ~200 m.

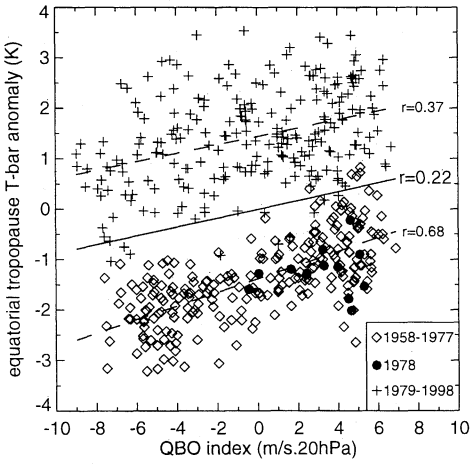

Figure 18. The 50-70 hPa $\overline{u}_{eq}$ shear anomaly plotted against the zonal mean equatorial tropopause temperature anomaly. The linear fit of the complete data set is plotted (solid line), and the correlation coefficient is indicated to the right. The fits for the 1958-1977 and 1979-1998 subsets of the data are plotted with dashed lines, and their correlation coefficients are indicated to their right.

The zonally averaged tropopause variations are somewhat smaller than those observed in individual station data; the observed peak-to-peak variation is ~2-3 K and ~300 m (~5.4 hPa) [*Reid and Gage*, 1985]. While zonal averages should be somewhat smaller than some local values, it has also been suggested [*Pawson and Fiorino*, 1998a, b, and 1999; *Randel et al.*, 1999] that the weaker QBO signal is due to the nature of a reanalysis product and is not specific to the NCEP reanalyses; a model will tend to flatten strong gradients, and the smaller shear and acceleration zone asymmetries seen in the NCEP data may also be produced by the model. However, it appears that although the amplitude of the oscillation and the asymmetries between the phases are somewhat weaker in the reanalyses than in the station data, the oscillation is well represented qualitatively.

7. Summary and Conclusion

The NCEP reanalysis data set, by covering 5 decades, provides a valuable record of interannual variability. It captures the essential nature of the QBO and more subtle phenomena documented previously: general latitudinal structure, thermal wind balance, shear zone asymmetry, and phase lock with the annual cycle. Because of the long time series and global coverage, some expected but previously undetected QBO signals can be seen fairly easily in the NCEP reanalysis, such as the meridional flow pattern. A new QBO indexing method is introduced. The primary index is based on the departure from the annual cycle of equatorial zonal mean zonal wind shear between 50 and 70 hPa and should be useful for studying global QBO variability near the tropopause.

The structure of the QBO is presented in three different ways. First, data are binned according to W, E, or intermediate phases of the QBO. The "W minus E" anomaly maps highlight the meridional-vertical structure of the QBO as it descends. This method, however, by averaging over time within each phase of the QBO, obscures some of the phase subtleties. A second view is obtained by using the compositing method of *Dunkerton and Delisi* [1985], where a composite QBO is constructed by averaging together many QBO cycles keying on "zero months" when the QBO index is zero. This provides a more precise view of meridional and vertical phase relationships. The third view employs a compositing method similar to that of *Yasunari* [1989], in which an "average W to E (or E to W) transition year" is created by averaging all the calendar years

during which that transition took place. Results include verification of the clustering of QBO zero wind line transitions at 50 hPa during the northern summer, persistent high-latitude effects, a stronger QBO circulation extension into the NH, temporal and spatial phase asymmetries, and a first direct comparison of the zonal wind range of the annual and QBO cycles. Future work will include exploration of the relative contribution of observations and assimilation balance constraints in determining the QBO meridional circulation in the NCEP reanalyses. Initial examination of individual QBO cycles shows much less coherent meridional circulation than the long-term composite, suggesting that the features are not entirely due to balance constraints in the assimilation process.

The QBO, as depicted in the NCEP reanalysis data, exhibits a discontinuity around 1978 that manifests itself in several different ways. After 1978, tropopause temperatures are 2-4 K warmer in the tropics and southern oceans [*Pawson and Fiorino*, 1999; *Randel et al.*, 2000], possibly because of the introduction of nadir sounding satellite temperature data. Tropopause pressures are smaller in the SH by up to 4 hPa and larger in the NH. Perhaps most significantly, the size of the QBO signal exhibits a sudden change in some fields and reduced intervariable consistency. Like the tropopause temperature and pressure, the temperature and geopotential height fields exhibit a decrease in the QBO signal after 1978, while the zonal wind signal seems unaffected and the meridional wind signal increases.

For example, the QBO variation in tropopause temperature is illustrated in Figure 18. Here the zonally averaged equatorial tropopause temperature anomaly is plotted against the primary QBO index (50-70 hPa $\overline{u}_{\mathrm{eq}}$ shear anomaly). Note the much warmer tropopause after 1978: this is most pronounced in the 100 hPa and tropopause temperature fields and is evident upward through the stratosphere. Also, the correlation coefficient between the QBO index and the zonally averaged tropopause temperature anomaly drops from 0.68 to 0.37 after 1978. Thus the QBO accounts for a significant portion of the interannual variability in tropopause temperature, but apparently less of it after 1978!

These two changes have been found by other authors [*Pawson and Fiorino*, 1999; *Randel et al.*, 2000]. It is likely that the introduction of nadir sounding temperature data to the NCEP data stream blunted the tropopause considerably and may have caused spurious changes in circulation features elsewhere. The QBO amplitude, correlation coefficient, and intervariable coherence near the tropopause seem more robust prior to 1978, and may thus be more accurate. An alternative explanation, however, is that there was a true regime shift in the general circulation near 1978. This is suggested by studying a variety of indicators, including the extent of ice in the Bering Sea and sea level pressure in the North Pacific [*Niebauer*, 1998], fisheries, timing of lake freezing in northern Canada, and a step reduction in mean ENSO index and other global circulation indices [*Ebbesmeyer et al.*, 1991; *Trenberth and Hurrel*, 1994; *Zhang et al.*, 1997]. The results reported herein are qualitatively valid for both pre- and post-1978 data; however, the change in QBO signal is cause for concern and is under further investigation by the authors.

Ultimately, it is of interest to determine the extent of the influence of the QBO on global weather. This work was originally undertaken as a part of a continuing investigation of the possibility that the stratospheric QBO modulates tropical deep convection. Results based on comparing NCEP fields, outgoing longwave radiation, and highly reflective cloud data will be reported elsewhere, focusing on modulation of regional and seasonal structures near the tropical tropopause by the QBO.

Acknowledgments. The authors would like to thank David Martin, Christopher Collimore, and three anonymous reviewers for useful conversations and suggestions, Barbara Naujokat for providing the Singapore wind data, and Charles Zender for his netCDF operators and supporting documentation. This research was made possible through a grant from the National Science Foundation grant ATM-9812429.

References

Alexander, M. J., and J. R. Holton, A model study of zonal forcing in the equatorial stratosphere by convectively induced gravity waves, *J. Atmos. Sci., 54*, 408-419, 1997.

Andrews, D. G., J. R. Holton, and C. B. Leovy, *Middle Atmosphere Dynamics*, 489 pp., Academic, San Diego, Calif., 1987.

Angell, J. K., Evidence of a relation between El Niño and QBO, and for an El Niño in 1991-92, *Geophys. Res. Lett., 19*, 285-288, 1992.

Bevington, P. R., and D. K. Robinson, *Data Reduction and Error Analysis for the Physical Sciences, 2nd Ed.*, pp. 53-57, McGraw-Hill, New York, 1992.

Chen, W., and R. Huang, The modulation of planetary wave propagation by the tropical QBO zonal winds and the associated effects in the residual meridional circulation, *Contrib. Atmos. Phys., 72*, 187-204, 1999.

Collimore, C. C., M. H. Hitchman, and D. W. Martin, Is there a quasi-biennial oscillation in tropical deep convection?, *Geophys. Res. Lett., 25*, 333-336, 1998.

Cordero, E. C., S. R. Kawa, and M. R. Schoeberl, An analysis of tropical transport: Influence of the quasi-biennial oscillation, *J. Geophys. Res., 102*, 16,453-16,462, 1997.

Doherty, G. M., R. E. Newell, and E. F. Danielsen, Radiative heating rates near the stratospheric fountain, *J. Geophys. Res., 89*, 1380-1384, 1984.

Dunkerton, T. J., A two-dimensional model of the quasi-biennial oscillation, *J. Atmos. Sci., 42*, 1151-1160, 1985.

Dunkerton, T. J., Non-linear Hadley circulation driven by asymmetric differential heating, *J. Atmos. Sci., 46*, 956-974, 1989.

Dunkerton, T. J., The role of gravity waves in the quasi-biennial oscillation, *J. Geophys. Res., 102*, 26,053-26,076, 1997.

Dunkerton, T. J., and D. P. Delisi, Climatology of the equatorial lower stratosphere, *J. Atmos. Sci., 42*, 376-396, 1985.

Dunkerton, T. J., and D. P. Delisi, Interaction of the quasi-

biennial oscillation and stratopause semiannual oscillation, *J. Geophys. Res., 102*, 26,107-26,116, 1997.

Ebbesmeyer, C., D. R. Cayan, D. R. McLain, F. H. Nichols, D. H. Peterson, and K. T. Redmond, 1976 step in the Pacific climate: Forty environmental changes between (1968-1975 and 1977-1984), in *Proceedings of the Seventh Annual Pacific Climate Workshop, April 1990*, edited by J. L. Betancourt and V. L. Sharp, *Tech. Rep. 26*, pp. 129-141, Calif. Dep. of Water Resour. Interagency Ecol. Stud. Program, Sacramento, 1991.

Garcia, R. R., and S. Solomon, A possible relationship between interannual variability in Antarctic ozone and the quasi-biennial oscillation, *Geophys. Res. Lett., 14*, 848-851, 1987.

Gray, L. J., and T. J. Dunkerton, The role of the seasonal cycle in the quasi-biennial oscillation of ozone, *J. Atmos. Sci., 47*, 2429-2451, 1990.

Gray, L. J., and S. Ruth, The modeled latitudinal distribution of the ozone quasi-biennial oscillation using observed equatorial winds, *J. Atmos. Sci., 50*, 1033-1046, 1993.

Gray, W. M., Atlantic seasonal hurricane frequency, Part 1: El Niño and 30 hPa quasi-biennial oscillation influences, *Mon. Weather Rev., 112*, 1649-1668, 1984.

Gray, W. M., C. W. Landsea, P. W. Mielke Jr., and K. J. Berry, Predicting atlantic seasonal hurricane activity 6-11 months in advance, *Weather Forecasting, 7*, 440-455, 1992a.

Gray, W. M., J. D. Sheaffer, and J. A. Knaff, Influence of the stratospheric QBO on ENSO variability, *J. Meteorol. Soc. Jpn., 70*, 975-995, 1992b.

Groves, G. V., Meridional wind quasi-biennial oscillations at 25-60 km altitude, 1962-1969, *J. Atmos. Terr. Phys., 37*, 1469-1475, 1975.

Hamilton, K., Mean wind evolution through the quasi-biennial cycle in the tropical lower stratosphere, *J. Atmos. Sci., 41*, 2113-2125, 1984.

Hamilton, K., and J. D. Mahlman, General circulation model simulation of the semiannual oscillation of the tropical middle atmosphere, *J. Atmos. Sci., 45*, 3212-3235, 1988.

Hitchman, M. H., and C. B. Leovy, Estimation of the Kelvin wave contribution to the semiannual oscillation, *J. Atmos. Sci., 45*, 1462-1475, 1988.

Hitchman, M. H., M. McKay, and C. R. Trepte, A climatology of stratospheric aerosol, *J. Geophys. Res., 99*, 20,689-20,700, 1994.

Hitchman, M. H., et al., Mean winds in the tropical stratosphere and mesosphere during January 1993, March 1994, and August 1994, *J. Geophys. Res., 102*, 26,033-26,052, 1997.

Holton, J. R., *An Introduction to Dynamic Meteorology*, 511 pp., Academic, San Diego, Calif., 1992.

Holton, J. R., and R. S. Lindzen, An updated theory for the quasi-biennial cycle of the tropical stratosphere, *J. Atmos. Sci., 29*, 1076-1080, 1972.

Holton, J. R., and H.-C. Tan, The influence of the equatorial quasi-biennial oscillation on the global circulation at 50 mb, *J. Atmos. Sci., 37*, 2200-2208, 1980.

Holton, J. R., P. H. Haynes, M. E. McIntyre, A. R. Douglass, R. B. Rood, and L. Pfister, Stratosphere-troposphere exchange, *Rev. Geophys., 33*, 403-439, 1995.

Kalnay, E., et al., The NCEP/NCAR 40-year reanalyses project, *Bull. Am. Meteorol. Soc., 77*, 437-471, 1996.

Kane, R. P., Relationship between QBOs of stratospheric winds, ENSO variability and other atmospheric parameters, *Int. J. Climatol., 12*, 435-447, 1992.

Kane, R. P., Quasi-biennial and quasi-triennial oscillations in the summer monsoon rainfall of the meteorological subdivisions of India, *Mon. Weather Rev., 123*, 1178-1184, 1995.

Kawamura, R., Quasi-biennial oscillation modes appearing in the tropical sea water temperature and 700 mb zonal wind, *J. Meteorol. Soc. Jpn., 66*, 955-965, 1988.

Kinnersley, J. S., Seasonal asymmetry of the low- and middle-latitude QBO circulation anomaly, *J. Atmos. Sci., 56*, 1140-1153, 1999.

Kinnersley, J. S., and S. Pawson, The descent rates of the shear zones of the equatorial QBO, *J. Atmos. Sci., 53*, 1937-1949, 1996.

Kinnersley, J. S., and K. K. Tung, Mechanisms for the extratropical QBO in circulation and ozone, *J. Atmos. Sci., 56*, 1942-1949, 1999.

Kistler, R., et al., The NCEP-NCAR reanalysis: Monthly means CD-ROM and documentation, *Bull. Am. Meteorol. Soc., 82*, 247-267, 2001.

Knaff, J. A., Evidence of a stratospheric QBO modulation of tropical convection, Pap. 510, Dept. of Atmos. Sci., Colorado State University, Ft. Collins, CO, 1992.

Lait, L. R., M. R. Schoeberl, and P. A. Newman, Quasi-biennial modulation of the Antarctic ozone depletion, *J. Geophys. Res., 94*, 11,559-11,571, 1989.

Lindzen, R. S., and J. R. Holton, A theory of the quasi-biennial oscillation, *J. Atmos. Sci., 25*, 1095-1107, 1968.

Mahlman, J. D., and S. B. Fels, Antarctic ozone decreases: A dynamical cause?, *Geophys. Res. Lett., 13*, 1316-1319, 1986.

Naujokat, B., An update of the observed quasi-biennial oscillation of the stratospheric winds over the tropics, *J. Atmos. Sci., 43*, 1873-1877, 1986.

Newell, R. E., and S. Gould-Stewart, A stratospheric fountain?, *J. Atmos. Sci., 38*, 2789-2796, 1981.

Niebauer, H. J., Variability in Bering Sea ice cover as affected by a regime shift in the North Pacific in the period 1947-1996, *J. Geophys. Res., 103*, 27,717-27,737, 1998.

O'Sullivan, D., and T. J. Dunkerton, The influence of the quasi-biennial oscillation on global constituent distributions, *J. Geophys. Res., 102*, 21,731-21,743, 1997.

O'Sullivan, D., and M. L. Salby, Coupling of the quasi-biennial oscillation and the extratropical circulation in the stratosphere through planetary wave transport, *J. Atmos. Sci., 47*, 650-673, 1990.

Pawson, S., and M. Fiorino, A comparison of reanalyses in the tropical stratosphere, Part 1: Thermal structure and the annual cycle, *Clim. Dyn., 14*, 631-644, 1998a.

Pawson, S., and M. Fiorino, A comparison of reanalyses in the tropical stratosphere, Part 2: The quasi-biennial oscillation, *Clim. Dyn., 14*, 645-658, 1998b.

Pawson, S., and M. Fiorino, A comparison of reanalyses in the tropical stratosphere, Part 3: Inclusion of the pre-satellite data era, *Clim. Dyn., 15*, 241-250, 1999.

Plumb, R. A., and R. C. Bell, A model of the quasi-biennial oscillation on an equatorial beta-plane, *Q. J. R. Meteorol. Soc., 108*, 335-352, 1982.

Plumb, R. A., and A. D. McEwan, The instability of a forced standing wave in a viscous stratified fluid: A laboratory analogue of the quasi-biennial oscillation, *J. Atmos. Sci., 35*, 1827-1839, 1978.

Politowicz, P. A., and M. H. Hitchman, Exploring the effects of forcing quasi-biennial oscillations in a two-dimensional model, *J. Geophys. Res., 102*, 16,481-16,497, 1997.

Randel, W. J., F. Wu, J. M. Russell III, A. Roche, and J. W. Waters, Seasonal cycles and QBO variations in stratospheric CH_4 and H_2O observed in UARS HALOE data, *J. Atmos. Sci., 55*, 163-185, 1998.

Randel, W. J., F. Wu, R. Swinbank, J. Nash, and A. ONeill, Global QBO circulation derived from UKMO stratospheric analyses, *J. Atmos. Sci., 56*, 457-474, 1999.

Randel, W. J., F. Wu, and D. J. Gaffen, Interannual variability of the tropical tropopause derived from radiosonde data and NCEP reanalyses, *J. Geophys. Res., 105*, 15,509-15,523, 2000.

Reed, R. J., The present status of the 26-month oscillation, *Bull. Am. Meteorol. Soc., 46*, 374-387, 1965.

Reed, R. J., W. J. Campbell, L. A. Rasmusson, and D. G. Rogers, Evidence of the downward-propagating annual wind reversal in the equatorial stratosphere, *J. Geophys. Res., 66*, 813-818, 1961.

Reid, G. C., and K. S. Gage, Interannual variations in the height of the tropical tropopause, *J. Geophys. Res., 90*, 5629-5635, 1985.

Trenberth, K. E., 1992: Global analyses from ECMWF and atlas of 1000 to 100 mb circulation statistics. *NCAR Tech. Notes NCAR/TN-373+STR.*, 191 pp., Natl. Cent. for Atmos. Res., Boulder, Colo., 1992.

Trenberth, K. E., and J. W. Hurrell, Decadal atmosphere-ocean variations in the Pacific, *Clim. Dyn., 9*, 303-319, 1994.

Trepte, C. R., and M. H. Hitchman, Tropical stratospheric circulation deduced from satellite aerosol data, *Nature, 355*, 626-628, 1992.

Tung, K. K., and H. Yang, Global QBO in circulation and ozone, Part 1: Reexamination of observational evidence, *J. Atmos. Sci., 51*, 2699-2707, 1994a.

Tung, K. K., and H. Yang, Global QBO in circulation and ozone, Part 2: A simple mechanistic model, *J. Atmos. Sci., 51*, 2708-2721, 1994b.

Veryard, R. G., and R. A. Ebdon, Fluctuations in the tropical stratospheric winds, *Meteorol. Mag., 90*, 125-143, 1961.

Wallace, J. M., General circulation of the tropical lower stratosphere, *Rev. Geophys., 11*, 191-222, 1973.

Whitney, L. D., and J. S. Hobgood, The relationship between sea surface temperatures and maximum intensities of tropical cyclones in the eastern North Pacific Ocean, *J. Clim., 10*, 2921-2930, 1997.

Xu, J.-S., On the relationship between the stratospheric quasi-biennial oscillation and the tropospheric Southern Oscillation, *J. Atmos. Sci., 49*, 725-734, 1992.

Yao, C.-Y., Geographical variation in the annual and quasi-biennial cycles in the tropical lower stratosphere, M.S. thesis, 130 pp., Univ. of Wisconsin-Madison, 1994.

Yasunari, T., A possible link of the QBOs between the stratosphere, troposphere and sea surface temperature in the tropics, *J. Meteorol. Soc. Jpn., 67*, 483-493, 1989.

Zawodny, J. M., and M. P. McCormick, Stratospheric Aerosol and Gas Experiment II measurements of the quasi-biennial oscillations in ozone and nitrogen dioxide, *J. Geophys. Res., 96*, 9371-9377, 1991.

Zhang, Y., J. M. Wallace, and D. S. Battisti, ENSO-like interdecadal variability: 1900-93, *J. Clim., 10*, 1004-1020, 1997.

A. S. Huesmann and M. H. Hitchman, Department of Atmospheric and Oceanic Sciences, University of Wisconsin-Madison, 1225 W. Dayton Street, Madison, WI 53706. (e-mail: amihan@xena.meteor.wisc.edu; matt@meteor.wisc.edu)

(Received July 7, 2000; revised November 1, 2000; accepted January 4, 2001.)